Frequency Decomposition-Based High-Performance Demura Processing with Low Memory Cost

Pilseung Heo, Dohoon Lee, Sewhan Na, Hyun-Wook Lim

***System LSI Division, Samsung Electronics Co. Ltd., Hwaseong, Korea**

Abstract

In this paper, we propose a new demura method for constructing display mura profiles by decomposing sampled mura data from the entire gray level into representative high spatial frequency components and multiple low spatial frequency components. By effectively allocating the components during demura processing, we achieved 98.5% in luminance uniformity while maintaining the color accuracy. This approach allows for implementation with 65.6% reduced memory size for compensation data storage compared to the conventional method, making it more cost-efficient in the display driver IC (DDIC).

Author Keywords

Demura; Spatial Frequency Decomposition; OLED;

1. Introduction

Mura in OLED displays of mobile devices is a critical factor in mass production yields, and various algorithms have been introduced to detect and compensate for it [1]. Figure 1 shows the conventional demura offset processing, where a high-resolution camera captures uncompensated mura condition at a few sampled gray levels and then demura algorithm makes mura offset layers using camera-captured information [2]. The demura algorithm interpolates few mura offsets to compensate for the entire gray level range. Typically, since the uncompensated mura condition at all gray levels contains fine stain information called sandy mura [3], these offset layers require a large amount of data capacity.To eliminate not only rough cloudy mura but also fine sandy mura, a significant amount of compensation data is required, leading to the proposal of mura map compression techniques to reduce memory usage [4].

In this paper, we classify mura profiles into sandy and cloudy types and examine their characteristics. We then propose an efficient compensation method under limited memory usage that enhances the luminance uniformity and color accuracy of the display.

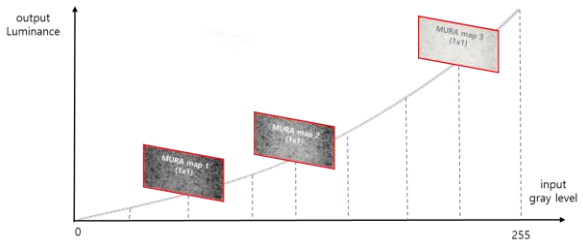

Figure 1. Conventional mura map allocation across a range of gray levels

2. Proposed Method

Spatial Frequency Decomposition: To analyze the mura profile of a real display panel, we first captured an image of the panel using a camera. The captured image was then processed using a low-pass filter (LPF) to extract the low-frequency components of the mura profile. LPF is used to remove high-frequency noise from an image while preserving the low-frequency details. In this case, we used a 3x3 box filter to perform the low-pass filtering. The filtered image was then subtracted from the original image to obtain the high-frequency components of the mura profile.

Figure 2(a) shows the original mura profile, while Figure 2(b) shows the mura profile after LPF. As can be seen, the LPF has removed most of the high-frequency noise, leaving only the low-frequency components of the mura profile. Figure 3 illustrates the changes in mura profile at the gray levels of 32 and 255. It can be observed that the low-frequency cloudy stain varies differently depending on the gray level, while the high-frequency sandy stain is distributed randomly but exhibits a similar pattern across the gray levels.

(a) Original mura profile (cloudy and sandy) (b) Low-pass filtered profile (cloudy)

Figure 2. Camera-captured original mura profile and its low-pass filtering result

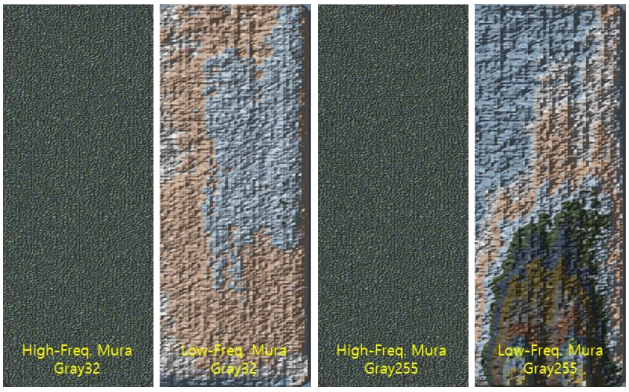

(a) sandy (b) cloudy (c) sandy (d) cloudy

Figure 3. Mura profile variation at the gray levels of 32 (a)(b) and 255 (c)(d) with high-frequency (a)(c) and low-frequency (b)(d)

Table 1 shows the correlation between the gray levels of 32 and 255 at high- and low-frequency components. The correlation coefficient (R) is calculated using the formula (1):

ISSN 0097-996X/25/5601-0366-$1.00 © 2025

$$R = \frac{n\sum XY - \sum X \sum Y}{\sqrt{\left(n\sum X^2 - (\sum X)^2\right) \cdot \left(n\sum Y^2 - (\sum Y)^2\right)}} \quad (1)$$

where n is the number of data points in the profile, X and Y are low and high-frequency components respectively.

Table 1. Comparison of the correlation coefficients (R) between the gray levels of 32 and 255 at the low- and high-frequency components

Component	RED pixel profile	GREEN pixel profile	BLUE pixel profile
Low-frequency	0.2113	0.2196	0.1936
High-frequency	0.9884	0.9848	0.9714

As shown in the table, the correlation between low-frequency components at 32 gray levels and low-frequency components at 255 gray levels is relatively low (R = 0.21). This indicates that there is no strong correlation between low-frequency cloudy patterns as the gray level changes. On the other hand, the correlation between high-frequency components of 32 and 255 gray levels is higher (R = 0.98), which suggests that high-frequency sandy patterns maintain a strong correlation regardless of changes in gray levels. This information can be useful in developing algorithms for mura compensation, as it provides insights into the relationship between the mura patterns and the gray levels of the display panel.

Decomposition-Based Demura Processing: Based on the analysis of the mura profile characteristics according to the frequency components, we propose the following demura processing approach:

1. High-Frequency Components: The correlation between high-frequency components is very high. Therefore, compensation for the high-frequency components can be processed using a single mura map with a relatively high spatial resolution across the full range of gray levels.

2. Low-Frequency Components: The correlation between low-frequency components is relatively low. To effectively process compensation for the low-frequency components, several different mura maps with relatively low spatial resolutions should be used, each corresponding to a sampled gray level.

This approach can be visualized in Figure 4, which illustrates the allocation of a representative 1x1 block size full-resolution single mura map and the application of 10 highly compressed mura maps for the sampled gray levels.

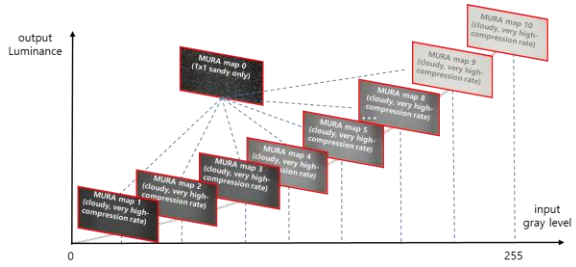

Figure 4. Proposed mura map allocation across a range of gray levels with a single sandy mura map of 'no-compressed' and 10 cloudy mura maps of 'very high compression rate'

3. Experiment and Results

To verify our approach, we implemented a demura algorithm on the FPGA with OLED module. Figure 5 shows the overall data flow of the image in the FPGA test environment. The demura block, which is divided into Image Gen-A and Gen-B and connected in series, generates a 36-bit image (R/G/B x 12 bits). Image Gen-A generates an inverse image of low-frequency components for compensation of cloudy mura, while Image Gen-B generates an inverse image of high-frequency components for compensation of sandy mura.

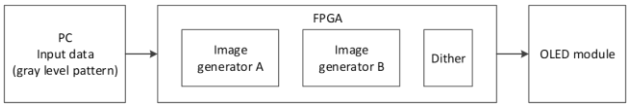

Figure 5. FPGA and OLED module environment for experiment

To evaluate the performance of the proposed demura algorithm, we compared it with a conventional demura algorithm in terms of display uniformity. The results are shown in Figure 6(a). As can be seen, the proposed demura algorithm significantly improved the display uniformity compared to the conventional algorithm, especially in the low and high gray levels where the conventional algorithm did not provide satisfactory results. This improvement can be attributed to the frequency decomposition-based compensation method, which takes into account the different characteristics of high- and low-frequency mura components.

The display uniformity is calculated using the formula (2):

$$Uniformity_{Lv} = \frac{Min_{Lv}}{Max_{Lv}} \times 100\% \quad (2)$$

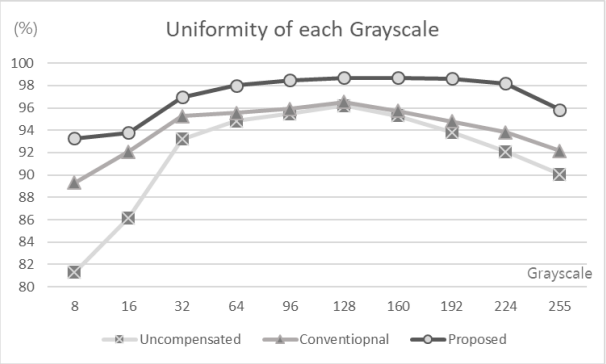

(a) Measured luminance uniformity

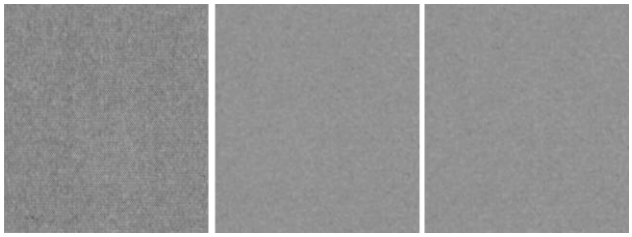

(b) Uncompensated (c) Conventional(after) (d) Proposed(after)

Figure 6. Display uniformity comparisons after compensation using conventional and proposed demura algorithm

Subjective evaluations were also conducted to further assess the effectiveness of the proposed algorithm in reducing sandy mura, which is not accurately measured by a colorimeter. Figure 6 (b), (c) and (d) show pictures taken of the sandy mura compensation results for an actual OLED display. The proposed can be seen in the picture to have similar performance compared to the conventional method, which is consistent with the subjective evaluation results - Mean Opinion Score (MOS) (5: excellent, 4: good, 3: fair, 2: poor, 1: bad), summarized in Table 2.

Table 2. Result of Subjective Evaluation on Sandy Mura

Evaluate on Sandy	Uncompensated	Conventional	Proposed
MOS	1.08	4.67	4.50

Through the experimental results, it was found that the newly proposed method showed superior performance in uniformity for each gray level while maintaining comparable performance to the existing method in terms of cognitive Sandy Mura compensation. In addition, an economic advantage can be seen in terms of the size of the reference data for Mura compensation, although we could not confirm the size of the Mura compensation data for the experimental panel, if we assume that multiple reference data are configured with a size of 1x1 or 2x2 based on the size of the sandy Mura of the corresponding mobile OLED panel, the following memory size gains can be obtained.

1. If it is said that the existing method uses three 1x1 compensation reference maps, two of the remaining 1x1 maps can be replaced with ten highly compressed (1/32) maps in addition to one 1x1 map. This means that data storage can be reduced by up to 54.2% compared to the existing method.

2. If it is said that in the existing method, two 2x2 compensation reference maps are used, then in addition to one 2x2 map, the remaining 2x2 map can be replaced with ten highly compressed (1/32) maps. This means that data storage can be reduced by up to 65.6% compared to the existing method.

Therefore, if the proposed method in the text is applied, it will be possible to obtain both the gain in uniformity performance and the h/w resource (memory capacity) gain at the same time.

4. Conclusion

In this paper, we analyzed the mura of a mobile OLED display by decomposing it into frequency components and proposed to allocate them appropriately during compensation. This allowed us to achieve improvements in both uniformity performance and hardware cost. The proposed approach is expected to serve as a foundation for meeting the recent demands for high-quality, low-cost demura solutions in DDIC.

5. References

[1] Kwon H, Park C, Kang K-S, Park J-H, Lee S-Y. “A Mura model-based optical compensation for organic light-emitting diode display luminance nonuniformity utilizing two image capturing”, J Soc. Inf. Display. (2025); 33(1): 24–33.

[2] Bo Magluyan, “Pixel Level Luminance Measurement and OLED Correction”, Soc. Inf. Display pp.1576-1578, (2017)

[3] Junjie Tang; Haoyuan Fan; Zifeng Wang; Yunzhi Wang; Zhengping Xiong; Dawei Ma; Fukun Sun, “AMOLED display Sandy Mura study and improvement”, Soc. Inf. Display pp.619-622, (2024)

[4] Chang-Hoon Son, Chan-Yung Kim, Hyeon-Woon Shin, Ho-Min Lim, Ji-Won Lee, “A Novel Compression Algorithm using Machine Learning for Mura Compensation of OLED Panel”, J. Soc. Inf. Display pp.1593-1596, (2024)